

Surface-Initiated Poly(3-methylthiophene) as a Hole-Transport Layer for Polymer Solar Cells with High Performance

Liqiang Yang,[†] S. Kyle Sontag,[‡] Travis W. LaJoie,[§] Wentao Li,[§] N. Eric Huddleston,[‡] Jason Locklin,^{*,‡} and Wei You^{*,†,§}

[†]Curriculum in Applied Sciences and Engineering, University of North Carolina at Chapel Hill, Chapel Hill, North Carolina 27599-3287, United States

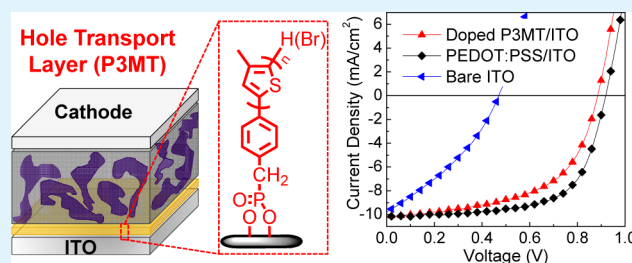
[‡]Department of Chemistry and College of Engineering, University of Georgia, Athens, Georgia 30602, United States

[§]Department of Chemistry, University of North Carolina at Chapel Hill, Chapel Hill, North Carolina 27599-3290, United States

S Supporting Information

ABSTRACT: In this work, uniform poly(3-methylthiophene) (P3MT) films are fabricated on indium–tin oxide (ITO) surfaces using surface-initiated Kumada catalyst-transfer polycondensation (SI-KCTP) from surface-bound arylnickel(II) bromide initiators. The P3MT interfacial layer is covalently bound to the ITO surface, thereby preventing possible delamination during the processing of additional layers. These surface-bound P3MT layers successfully serve as the hole-transport layer for solution-processed bulk heterojunction polymer solar cells. Efficiencies greater than 5% have been achieved on devices based on doped thin P3MT interfacial layers. Moreover, because of the excellent stability of the covalently immobilized P3MT on ITO substrates, devices based on reused P3MT/ITO substrates extracted from old devices exhibit efficiencies similar to those of the original devices.

KEYWORDS: conjugated polymers, solar cells, interfacial layers, polymer brushes, surface-initiated polymerization, Kumada catalyst-transfer polycondensation



Poly(3,4-ethylenedioxythiophene):poly(styrenesulfonate) (PEDOT:PSS) is a water-soluble polyelectrolyte system with good film-forming properties, high conductivity (ca. 10 S/cm), high visible-light transmittance, and excellent stability.¹ Because of these notable features, PEDOT:PSS has become one of the most widely used materials in organic electronics, including organic light-emitting diodes^{2,3} and organic photovoltaic devices.^{4,5} In the conventional bulk heterojunction (BHJ) polymer solar cells, PEDOT:PSS essentially serves as the standard interfacial modifier atop the ubiquitous indium–tin oxide (ITO) anode to improve both morphological and electronic figures of merit.⁶ However, a number of drawbacks with PEDOT:PSS have also been identified. Notably, the acidic nature of PEDOT:PSS can corrode the ITO electrode,^{7,8} leading to a chemical instability at the interface.⁹ Furthermore, PEDOT:PSS does not have sufficient electron-blocking capability,⁸ which could render electron leakage at the anode to reduce the short-circuit current density (J_{sc}) in polymer solar cells.

To address these challenges with PEDOT:PSS, a number of new materials have been tested as viable alternatives to modify the surface of the ITO anode in polymer solar cells.^{9,10} For example, Jo and co-workers employed a self-doped, grafted conductive copolymer (PSSA-g-PANI) as the hole-transport layer (HTL) in polymer solar cells.¹¹ The conductivity and

acidity of this copolymer can be easily tuned by varying the PSSA and PANI molar ratio. Devices based on PSSA-g-PANI exhibited an increased lifetime of more than 30-fold compared with PEDOT:PSS-based devices.¹² Still, the acidic and hygroscopic nature of these conducting polymers may lead to degradation problems similar to those found in PEDOT:PSS. Other attempted materials include thin films of carbon nanotubes, self-assembled monolayers, and transition-metal oxides (e.g., MoO_3 , V_2O_5 , NiO , and WO_3), with various degrees of success.^{13–22}

In our own pursuit of “PEDOT:PSS-free” anodes (with an ultimate goal of “ITO-free” anodes), conjugated polymer brushes attracted our attention because of a number of unique features. First, these conjugated polymer brushes can be covalently linked to the surface of many types of substrates,^{23–27} which provides excellent stability in both the neutral and doped states. Second, the chemical structures of these conjugated polymer brushes can be varied to offer “tunable” energy levels to facilitate charge transport from the BHJ blend to the anode.^{28,29} Third, these densely packed conjugated polymer brushes could further tune the interfacial

Received: July 20, 2012

Accepted: September 13, 2012

Published: September 13, 2012

energy at the electrode with potential improvement on the active layer morphology, particularly at the anode interface.

As a proof of concept to test the viability of these conjugated polymer brushes in replacing PEDOT:PSS, we synthesized poly(3-methylthiophene) (P3MT) films of various thicknesses from ITO surfaces using surface-initiated Kumada catalyst-transfer polycondensation (SI-KCTP) from surface-bound arylnickel(II) bromide initiators.^{28,29} When the P3MT interfacial layer was employed as the HTL for solution-processed BHJ polymer solar cells with a typical configuration of ITO/P3MT/polymer:phenyl-C61-butyric acid methyl ester (PCBM)/Ca/Al (Figure 1), we were able to obtain cell

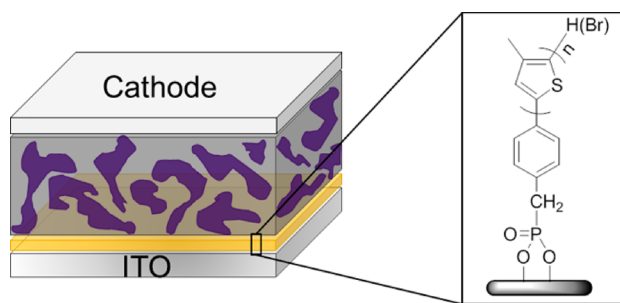


Figure 1. Device structure of the BHJ polymer solar cell based on the P3MT interfacial layer. The P3MT layer is covalently bound to the ITO surface using SI-KCTP. Covalent immobilization prevents delamination during the processing of additional layers. The bromine at the chain end demonstrates chain termination via possible intermolecular transfer of the nickel(0) catalyst.²⁸

efficiencies as high as 5% based on doped thin P3MT interfacial layers. Furthermore, this covalently bound P3MT interfacial layer offers *excellent stability*. As a result, photovoltaic devices based on reused P3MT/ITO substrates exhibit efficiencies similar to those obtained from solar cells with pristine P3MT/ITO substrates. All of these features indicate that surface-bound P3MT interfacial layer is a promising alternative to PEDOT:PSS as the HTL for polymer solar cells.

A successful HTL for polymer solar cells requires excellent optical transparency in order to minimize any loss of incident light. Figure 2a compares the optical transmittance of undoped P3MT on ITO substrates with that of a PEDOT:PSS-coated reference substrate. All of the undoped P3MT films exhibit excellent transparency at wavelengths of over 650 nm, similar to what Kiriy et al. observed for surface-bound poly(3-hexylthiophene) (P3HT) in the dry state.²⁷ However, the lowest transmittances of these undoped P3MT films appear at 450 nm, lower than those of P3HT films.²⁷ We attribute this to a combination of aggregation within the film and/or oligomeric P3MT that results from early chain termination.²⁸ While thinner P3MT films show exceptional transparency (e.g., over 95% transmittance for a 3 nm thin film) across the spectrum, increasing the thickness of P3MT attenuates the transmittance of the P3MT film (Figure 2a). For example, the 20-nm-thick P3MT film only offers a transmittance of 75% at 450 nm, which implies that P3MT layers over 20 nm thick may have a negative effect on the performance of solar cells because of a low transmittance. On the other hand, the optical transmittance of PEDOT:PSS (~40 nm) peaks (99.2%) at around 430 nm but continually decreases to 90% at 850 nm. Therefore, while PEDOT:PSS/ITO substrates might be slightly advantageous for applications targeting the visible region, surface-grown

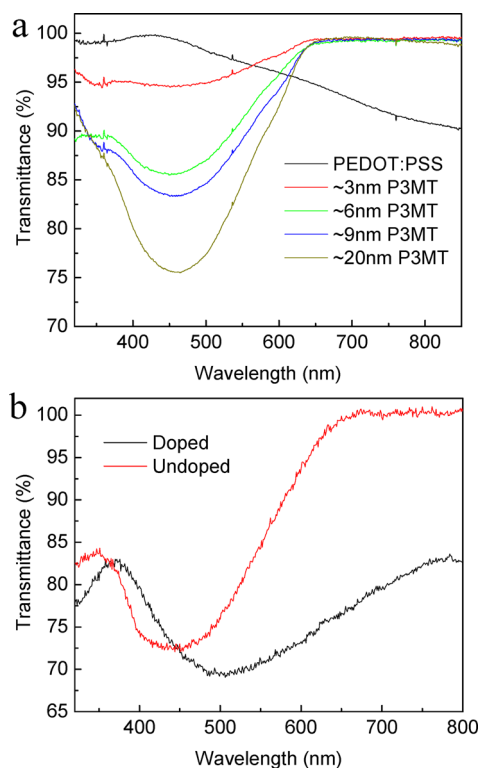


Figure 2. Transmission spectra for (a) the 40 nm PEDOT:PSS reference and a series of undoped P3MT layers with different thicknesses, all on ITO substrates, and (b) the P3MT layer (~20 nm) before and after doping.

P3MT/ITO outperforms PEDOT:PSS/ITO for applications requiring optical transparency extending into longer wavelength (e.g., small-band-gap polymer-based solar cells). Additionally, electrochemical doping of the P3MT film (a detailed doping procedure can be found in the Supporting Information) significantly decreases the transmittance of the film in the long-wavelength range (over 450 nm), with the maximum decrease in the transmittance red shifting to 500 nm (Figure 2b). This is indicative of polaronic and bipolaronic states along the P3MT backbone, leading to the observed red shift in the transmittance spectrum.²⁹

The “true” success of any HTL for polymer solar cells can only be verified in fabricated devices with careful design and proper control groups. In our experimental design, we selected two representative polymers, P3HT^{30–32} and PBnDT-DTfBT³³ (structures in Figure S2 in the Supporting Information), to test the general applicability of the P3MT film as a new HTL. These two polymers are largely different in energy levels and band gaps. The highest occupied molecular orbital (HOMO) energy level and optical band gap for P3HT are -5.2 and $+1.9$ eV,¹⁹ respectively, while corresponding values for PBnDT-DTfBT are -5.54 and $+1.7$ eV, respectively.³³ As for the control groups, we fabricated reference cells based on PEDOT:PSS/ITO and bare ITO substrates, in addition to cells based on P3MT/ITO substrates. Finally, two other factors, doped versus undoped and changes in the film thickness of the covalently bound P3MT, were also included in the experimental design.

Figure 3 presents the representative current–voltage (J – V) curves of test devices based on P3MT (9 nm)/ITO and reference cells, with key photovoltaic characteristics summar-

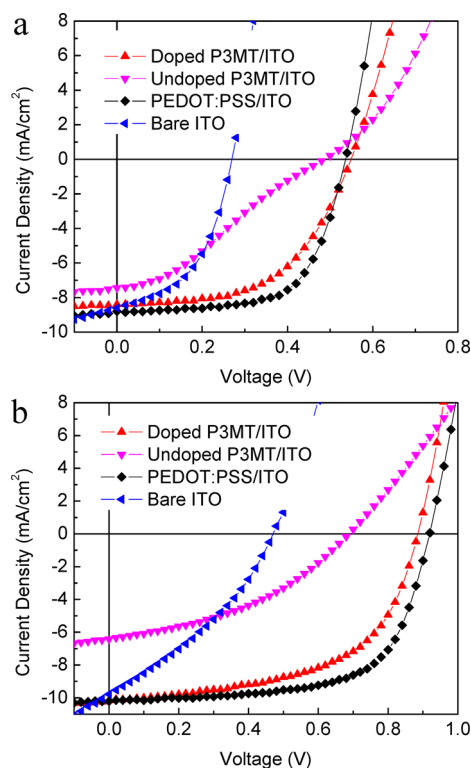


Figure 3. Characteristic J - V curves of the BHJ solar cell devices based on (a) P3HT and (b) PBnDT-DTfBT under one sun condition ($100 \text{ mW}/\text{cm}^2$).

ized in Table 1 and Table S1 in the Supporting Information. Compared with the reference devices based on bare ITO anodes, there is a noticeable increase in V_{oc} of all devices based on undoped P3MT/ITO substrates, ascribed to the modified work function of P3MT/ITO compared with that of the bare electrode. Unfortunately, the lower short-circuit current (J_{sc}) and fill factor (FF) of devices based on the undoped P3MT/ITO substrate attenuate the benefit of the increased V_{oc} , leading to a low efficiency similar to that of devices based on bare ITO. The low J_{sc} and FF of these devices based on undoped P3MT/ITO are largely attributed to the low mobility and poor charge transport in the undoped P3MT interfacial layer. These issues can be easily addressed via electrochemical doping of the P3MT interfacial layer. All of the devices based on doped P3MT interfacial layers exhibit much improved J_{sc} and V_{oc} , close to those obtained from the PEDOT:PSS reference cells (Figure 3). Doping improves V_{oc} and J_{sc} by inducing polaronic and bipolaronic states within the backbone of the polymer chains that facilitate charge transport. In addition, the relatively high LUMO level of P3MT inhibits electron transfer from the active layer to the ITO anode. Therefore, the doped P3MT interfacial layer can be considered as a hole-only transport layer for BHJ solar cells. Like PEDOT:PSS, this doped P3MT interfacial layer can work with a wide range of HOMO levels in various polymers (e.g., -5.2 eV in P3HT and -5.54 eV in PBnDT-DTfBT). We observed slightly lower FF in devices based on the doped P3MT, compared with those of PEDOT:PSS-based reference cells. This is likely due to the less efficient hole-collecting ability of the doped P3MT layer. These results imply that, after further optimization of the polymer orientation and electronic properties of these P3MT

Table 1. Photovoltaic Properties of Devices Based on Doped P3MT/ITO, PEDOT:PSS/ITO, and Bare ITO^a

polymer	interfacial layer (HTL)	V_{oc} (V)	J_{sc} (mA/cm^2)	FF (%)	η (%)
P3HT	N/A	0.27	8.61	48.4	1.12
	$\sim 3 \text{ nm}$ P3MT	0.45	6.81	47.5	1.46
	$\sim 6 \text{ nm}$ P3MT	0.49	7.45	55.1	2.03
	$\sim 9 \text{ nm}$ P3MT	0.55	8.39	54.5	2.51
	$\sim 20 \text{ nm}$ P3MT	0.47	5.81	46.5	1.27
	PEDOT:PSS	0.53	8.80	64.8	3.02
PBnDT-DTfBT	N/A	0.47	9.78	34.3	1.58
	$\sim 3 \text{ nm}$ P3MT	0.87	7.62	52.3	3.42
	$\sim 6 \text{ nm}$ P3MT	0.89	10.1	53.9	4.85
	$\sim 9 \text{ nm}$ P3MT	0.89	10.2	55.7	5.04
	$\sim 20 \text{ nm}$ P3MT	0.87	9.76	55.8	4.74
	PEDOT:PSS	0.91	10.2	65.6	6.09

^aAll polymers were blended with PCBM at a weight ratio of 1:1 in DCB.

interfacial layers,³⁴ the performance of related devices should be equal or superior to that of PEDOT:PSS-based devices.

Next, we investigated the impact of the thicknesses of P3MT interfacial layers on the photovoltaic properties of BHJ devices. Not surprisingly, for each studied thickness, the device based on doped P3MT (Table 1) exhibits a better performance than the device based on undoped P3MT (Table S1 in the Supporting Information). This is consistent with our previous discussion in that doping can significantly improve the charge transport through the P3MT layer, leading to better device characteristics. The best photovoltaic performance was observed in the device with a 9 nm P3MT interfacial layer (doped), regardless of which donor polymer was used (P3HT and PBnDT-DTfBT). When the film thickness is less than 5 nm, the P3MT film has a uniform morphology, but it is likely that the layer cannot be sufficiently doped, leading to relatively low FF and J_{sc} . On the other hand, thick P3MT layers (e.g., $\sim 20 \text{ nm}$) significantly reduce the transmittance of the P3MT/ITO substrate (Figure 2), thereby resulting in decreased J_{sc} . It appears that within our studied thicknesses, a $\sim 9\text{-nm}$ -thick P3MT layer strikes a balance between the hole transport and optical transparency, resulting in the highest possible efficiency in both P3HT- and PBnDT-DTfBT-based BHJ devices. Interestingly, J_{sc} of P3HT-based devices dramatically decreases from 8.4 to 5.8 mA/cm^2 when the thickness of the P3MT interfacial layer is increased from 9 to 20 nm. Meanwhile, only a small decrease of J_{sc} was observed in the PBnDT-DTfBT-based devices with the same variation of the thickness of the P3MT layers. This can be explained by the fact that the absorption of the doped P3MT interfacial layer is largely overlapped with the absorption of P3HT (Figure S3 in the Supporting Information), whereas the absorption of smaller-band-gap polymers, such as PBnDT-DTfBT, is much less impacted by the thickness of the P3MT layer. Therefore, the device of PBnDT-DTfBT based on a 20 nm P3MT interfacial layer still exhibits an efficiency as high as 4.7%, only 6% lower than that of the device with a 9 nm P3MT layer (over 5.0%).

Lastly, we tested the stability of these P3MT interfacial layers. PEDOT:PSS is intrinsically unstable because of its hygroscopic nature. It readily absorbs a trace amount of water, presenting a threat to the long-term stability of BHJ solar cells. Upon severe water uptake, PEDOT:PSS will delaminate the active layer from ITO, leading to catastrophic failure of the

device. On the contrary, because of covalent immobilization of these P3MT chains, the P3MT interfacial layers on ITO substrates offer excellent stability upon exposure to air, water, and organic solvents. As an extreme example, the P3MT/ITO substrates can even be reused for BHJ devices after removal of the polymer/PCBM active layer as well as the metal cathode. We used previously fabricated and tested devices (over 1 month after the initial device fabrication) based on 9 nm doped P3MT to demonstrate this stability. The devices were ultrasonicated for 20 min in hot *o*-dichlorobenzene (DCB) followed by acetone, deionized water, and then 2-propanol to clean all of the layers above the P3MT/ITO substrate. Half of the reused P3MT/ITO substrates were electrochemically doped, while no further treatment was applied to the other half, prior to the final step of device fabrication and testing. Representative J - V curves of devices based on these reused P3MT/ITO substrates with PBnDT-DTfBT as the donor polymer are shown in Figure 4. The efficiency of the device

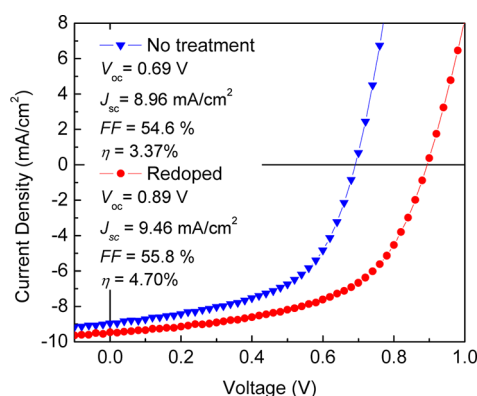


Figure 4. Characteristic J - V curves of the BHJ solar cell devices based on reused P3MT/ITO substrates under one sun condition (100 mW/cm^2).

based on reused P3MT/ITO substrate without additional doping is noticeably lower than that of the device on the original doped P3MT (5.0% in Table 1) but still much better than that of the device on pristine P3MT without any doping. This implies that charge transport through these reused P3MT films is not as efficient as that through the original doped layers, possibly because of the reduction and partial loss of counterions during the extensive cleaning process. Thus, not surprisingly, after electrochemical redoping of P3MT of these recycled substrates, the efficiency of related devices recovers to 4.7%, which is almost as high as that of the devices on the original doped P3MT layers. These results indicate that there is no irreversible damage to the P3MT layer during the cleaning procedure, which can be largely attributed to the covalent attachment of the P3MT layer to the ITO substrate.

In summary, we have successfully introduced surface-bound P3MT interfacial layers, grown via SI-KCTP, as a viable alternative HTL for solution-processed polymer solar cells. Devices based on this new HTL with semioptimized thickness upon doping demonstrate efficiencies comparable with those obtained from PEDOT:PSS-based devices. More importantly, unlike the acidic and hygroscopic PEDOT:PSS, which leads to chemical instability at the PEDOT:PSS/ITO interface, these surface-bound P3MT interfacial layers offer superior stability in air, water, and organic solvents (e.g., under sonication in hot DCB). One can even reuse the P3MT/ITO substrates from old

devices after stripping off the active layer and metal electrode, with the devices based on these “recycled” substrates exhibiting efficiencies as high as those of the original devices. Finally, the great tunability of these conjugated polymer brushes, e.g., the chemical structure, the length, the grafting density, and the doping methods, offers a wide variety of possibilities for further improvement and optimization. With all of these aforementioned features, the surface-bound conjugated polymer brushes are poised to be a very promising interfacial layer for organic electronics.

■ ASSOCIATED CONTENT

📄 Supporting Information

Experimental procedures, chemical structures of all polymers, UV-vis absorption spectra of all polymers, J - V curves of all devices, and tabulated photovoltaic properties of undoped P3MT-based devices. This material is available free of charge via the Internet at <http://pubs.acs.org>.

■ AUTHOR INFORMATION

Corresponding Author

*E-mail: jlocklin@uga.edu (J.L.), wyou@unc.edu (W.Y.).

Notes

The authors declare no competing financial interest.

■ ACKNOWLEDGMENTS

This work was supported by a collaborative grant from the NSF (Grant CHE-1058626). We also acknowledge financial support from the Office of Naval Research (Grant N000141110235). T.W.L. is supported by the NSF Graduate Research Fellowship under Grant DGE-1144081. W.Y. is a Camille Dreyfus Teacher-Scholar.

■ REFERENCES

- (1) Groenendaal, L.; Jonas, F.; Freitag, D.; Pielartzik, H.; Reynolds, J. R. *Adv. Mater.* **2000**, *12*, 481.
- (2) Elschner, A.; Bruder, F.; Heuer, H. W.; Jonas, F.; Karbach, A.; Kirchmeyer, S.; Thurm, S.; Wehrmann, R. *Synth. Met.* **2000**, *111–112*, 139.
- (3) Lane, P. A.; Kushto, G. P.; Kafafi, Z. H. *Appl. Phys. Lett.* **2007**, *90*, 023511.
- (4) Arias, A. C.; Granström, M.; Thomas, D. S.; Petritsch, K.; Friend, R. H. *Phys. Rev. B* **1999**, *60*, 1854.
- (5) Coffey, D. C.; Reid, O. G.; Rodovsky, D. B.; Bartholomew, G. P.; Ginger, D. S. *Nano Lett.* **2007**, *7*, 738.
- (6) Pingree, L. S. C.; MacLeod, B. A.; Ginger, D. S. *J. Phys. Chem. C* **2008**, *112*, 7922.
- (7) Wong, K. W.; Yip, H. L.; Luo, Y.; Wong, K. Y.; Lau, W. M.; Low, K. H.; Chow, H. F.; Gao, Z. Q.; Yeung, W. L.; Chang, C. C. *Appl. Phys. Lett.* **2002**, *80*, 2788.
- (8) Yan, H.; Lee, P.; Armstrong, N. R.; Graham, A.; Evmenenko, G. A.; Dutta, P.; Marks, T. J. *J. Am. Chem. Soc.* **2005**, *127*, 3172.
- (9) Ma, H.; Yip, H.-L.; Huang, F.; Jen, A. K. Y. *Adv. Funct. Mater.* **2010**, *20*, 1371.
- (10) Yip, H.-L.; Jen, A. K. Y. *Energy Environ. Sci.* **2012**, *5*, 5994.
- (11) Jung, J. W.; Lee, J. U.; Jo, W. H. *J. Phys. Chem. C* **2009**, *114*, 633.
- (12) Choi, M.-R.; Han, T.-H.; Lim, K.-G.; Woo, S.-H.; Huh, D. H.; Lee, T.-W. *Angew. Chem., Int. Ed.* **2011**, *123*, 6398.
- (13) Sun, Y.; Takacs, C. J.; Cowan, S. R.; Seo, J. H.; Gong, X.; Roy, A.; Heeger, A. J. *Adv. Mater.* **2011**, *23*, 2226.
- (14) Subbiah, J.; Kim, D. Y.; Hartel, M.; So, F. *Appl. Phys. Lett.* **2010**, *96*, 063303.
- (15) Kröger, M.; Hamwi, S.; Meyer, J.; Riedl, T.; Kowalsky, W.; Kahn, A. *Appl. Phys. Lett.* **2009**, *95*, 123301.

- (16) Tao, C.; Ruan, S. P.; Xie, G. H.; Kong, X. Z.; Shen, L.; Meng, F. X.; Liu, C. X.; Zhang, X. D.; Dong, W.; Chen, W. Y. *Appl. Phys. Lett.* **2009**, *94*, 043311.
- (17) Meyer, J.; Kroger, M.; Hamwi, S.; Gnam, F.; Riedl, T.; Kowalsky, W.; Kahn, A. *Appl. Phys. Lett.* **2010**, *96*, 193302.
- (18) Hayakawa, A.; Yoshikawa, O.; Fujieda, T.; Uehara, K.; Yoshikawa, S. *Appl. Phys. Lett.* **2007**, *90*, 163517.
- (19) Kim, J. Y.; Kim, S. H.; Lee, H. H.; Lee, K.; Ma, W.; Gong, X.; Heeger, A. J. *Adv. Mater.* **2006**, *18*, 572.
- (20) Sun, Y.; Seo, J. H.; Takacs, C. J.; Seifert, J.; Heeger, A. J. *Adv. Mater.* **2011**, *23*, 1679.
- (21) Yip, H.-L.; Hau, S. K.; Baek, N. S.; Ma, H.; Jen, A. K. Y. *Adv. Mater.* **2008**, *20*, 2376.
- (22) Bulliard, X.; Ihn, S.-G.; Yun, S.; Kim, Y.; Choi, D.; Choi, J.-Y.; Kim, M.; Sim, M.; Park, J.-H.; Choi, W.; Cho, K. *Adv. Funct. Mater.* **2010**, *20*, 4381.
- (23) Marshall, N.; Sontag, S. K.; Locklin, J. *Chem. Commun.* **2011**, *47*, 5681.
- (24) Kiriya, A.; Senkovskyy, V.; Sommer, M. *Macromol. Rapid Commun.* **2011**, *32*, 1503.
- (25) Marshall, N.; Sontag, S. K.; Locklin, J. *Macromolecules* **2010**, *43*, 2137.
- (26) Sontag, S. K.; Marshall, N.; Locklin, J. *Chem. Commun.* **2009**, 3354.
- (27) Senkovskyy, V.; Khanduyeva, N.; Komber, H.; Oertel, U.; Stamm, M.; Kuckling, D.; Kiriya, A. *J. Am. Chem. Soc.* **2007**, *129*, 6626.
- (28) Sontag, S. K.; Sheppard, G. R.; Usselman, N. M.; Marshall, N.; Locklin, J. *Langmuir* **2011**, *27*, 12033.
- (29) Doubina, N.; Jenkins, J. L.; Paniagua, S. A.; Mazzio, K. A.; MacDonald, G. A.; Jen, A. K. Y.; Armstrong, N. R.; Marder, S. R.; Luscombe, C. K. *Langmuir* **2012**, *28*, 1900.
- (30) He, M.; Han, W.; Ge, J.; Yang, Y.; Qiu, F.; Lin, Z. *Energy Environ. Sci.* **2011**, *4*, 2894.
- (31) He, M.; Qiu, F.; Lin, Z. *J. Mater. Chem.* **2011**, *21*, 17039.
- (32) He, M.; Han, W.; Ge, J.; Yu, W.; Yang, Y.; Qiu, F.; Lin, Z. *Nanoscale* **2011**, *3*, 3159.
- (33) Zhou, H.; Yang, L.; Stuart, A. C.; Price, S. C.; Liu, S.; You, W. *Angew. Chem., Int. Ed.* **2011**, *50*, 2995.
- (34) Huddleston, N. E. S.; Sontag, S. K.; Bilbrey, J. A.; Sheppard, G. R.; Locklin, J. *Macromol. Rapid Commun.* **2012**, DOI: DOI: 10.1002/marc.201200472.